

# Optimal Control of Reactive-Power Compensators in Industrial Networks – A Virtual Compensator Concept

Leopold Herman, Igor Papič

University of Ljubljana, Faculty of Electrical Engineering, Tržaška cesta 25, Ljubljana  
E-mail: poldi.herman@fe.uni-lj.si, igor.papic@fe.uni-lj.si

**Abstract.** In modern industrial processes, the number of nonlinear loads - known to be a major source of current harmonics - is constantly growing. At the same time, the number of reactive-power compensators operating in these networks is growing too. Though the compensators are not the source of harmonic distortions, they may cause high amplifications of harmonics by creating resonance conditions. This can cause malfunctions or even loss of equipment. Due to the increasing number of the reactive-power compensators operating in typical industrial networks, control of these networks is also becoming extremely demanding. An industrial network operator has a difficult task of finding an optimal configuration of compensators, meeting the reactive-power demands and at the same time not causing resonance amplifications of harmonics. The paper thus proposes a concept of a virtual compensator. It combines all the reactive-power devices of a certain network within a single control scheme. This enables the operator to control each compensator independently in real time and to achieve their optimal configuration at any operation point of the network. The effectiveness of the proposed algorithm is demonstrated on a realistic industrial-network model by means of simulations.

**Keywords:** Reactive-power compensation, optimisation, harmonics, resonance.

## 1 INTRODUCTION

Reactive-power compensation is an important issue in industrial power systems. Industrial loads impose varying active- and reactive-power demands, where the reactive-power has to be compensated in order to improve the power factor (PF) and efficiently deliver the active power to the loads. Usually, both the utilities and the customers are interested in improving PF at the customer-utility point of common coupling (PCC). This permits the customers to benefit from reduced system losses, released transmission capacity and improved voltage profile, moreover, the electric-bill is decreased, since utilities penalise customers for their poor PF. The extent of these benefits depends mainly on the location, size, type, and number of shunt compensators and also on their control settings [1,2].

Optimal capacitor bank placement and sizing under sinusoidal conditions is a well-researched problem. In the extensive literature covering this topic, different methods of finding an optimal solution are presented, most of them giving very good results. The methods could be classified as follows: analytical, numerical programming, heuristic and those based on artificial intelligence [3-6]. In more recent papers, the presence of the voltage and current harmonics is also taken into

account [7-10]. Here, too, a wide variety of methods are being used for solving the nonlinear optimisation problem, such as genetic algorithms, fuzzy logic theory, etc. Many of these techniques are very fast in finding a solution, but may require a significant processing power. Efforts taken by the authors are therefore aimed towards finding the most suitable methods for solving the nonlinear optimisation problem, giving a solution (global optimum) quickly and with as few computational steps as possible.

In general, one can say that there is a considerable interest by researchers in the field of optimal compensator sizing and placement which, however, does not apply to control of these devices. Namely, very little attention is paid to the problem of optimal reactive-power control, accounting for the harmonics present in the network. This issue is particularly problematic due to the fact that in the last decade, a great increase in the number of adjustable-speed motor drives and a vast variety of other nonlinear loads used in industrial networks have been witnessed. At the same time, the number of reactive-power compensation devices operating in these networks is growing too, where most of them still being conventional passive compensators. Thus, more and more cases are being reported from industry on the problem of resonance amplification of harmonics. As the conventional passive compensator cannot be dynamically adjusted to the

variations in the network states, changed assumptions (network topology and electric-parameter values) taken into account when building the compensator, can quickly lead to incorrect operation. When the resonant frequency of the compensator aligns with the harmonic present in the network, the result can be overheating and shorter operational life of certain equipment (transformers, cables, compensators), occurrence of noise and vibrations (motors, generators), incorrect operation of certain devices (computers, printers) and in extreme cases, equipment failure or even destruction.

As there are in a typical industrial network several compensation devices connected to different voltage levels, the number of different combinations of the settings is considerable, but not all of them are appropriate in terms of the harmonic conditions in the network. It is therefore rather difficult for the operator to decide how to operate and predict all of the potentially dangerous situations. The task is very demanding already in steady state conditions, while during the system transient states it can become quite unmanageable.

The paper presents a concept of a virtual compensator to be used in solving the above issues of reactive-power compensation in industrial networks. The paper is organised as follows. In chapter 2, the phenomenon of resonance between the compensator and the network is presented in detail. Chapter 3 describes the basic idea of the proposed virtual compensator. Chapter 4 presents a model of a real industrial network. Results are given in chapter 5. In chapter 6, conclusions are drawn.

## 2 RESONANCE BETWEEN THE COMPENSATOR AND THE NETWORK

All electric circuits containing elements of an inductive and capacitive character have one or more resonance frequencies. The resonance between the compensator and the network occurs at a frequency at which the capacitive and inductive reactances of a system cancel each other out thus leaving resistivity in the system as the only form of impedance. At this frequency, high amplifications of the current and voltage harmonics can occur threatening to damage the installed compensators and other equipment in the network.

Figure 1 a) shows an equivalent circuit of an industrial feeder. The symbols used are:  $\underline{U}_S$  is the supply voltage (Thevenin voltage),  $\underline{Z}_S = R_S + jX_S$  is the supply impedance (Thevenin impedance),  $\underline{Z}_L = R_L + jX_{LL}$  is the load impedance,  $\underline{Z}_C = R + jX_L - jX_C$  is the compensator impedance,  $\underline{U}_C$  is the voltage at compensator PCC, and  $I_C$  is the compensator current.

The Thevenin voltage source representing the utility supply and the harmonic-current source representing the nonlinear load are:

$$\underline{U}_S = \underline{U}_{S,1} + \sum_{h=2}^n \underline{U}_{S,h} \quad (1)$$

and

$$\underline{I}_L = \underline{I}_{L,1} + \sum_{h=2}^n \underline{I}_{L,h}, \quad (2)$$

where  $h$  denotes the harmonic order.

For the utility equivalent (series) impedance, the following expression can be written (see Fig. 1 b):

$$\underline{Z}_{ser,h} = R_S + j \cdot h \cdot X_{S,1} + R + j \cdot h \cdot X_{L,1} - j \cdot \frac{X_{C,1}}{h} \quad (3)$$

Neglecting the compensator resistance and reactance at the  $h^{th}$  harmonic, we get:

$$\underline{Z}_{ser,h} \approx R_S + j \cdot h \cdot X_{S,1} - j \frac{X_{C,1}}{h}, \quad (4)$$

$$\underline{Z}_{ser}^{f_{r-s}} \approx R_S. \quad (5)$$

Equivalent system and compensator impedances coupled in series becomes very small near series resonance point  $f_{r-s}$  and limited downward only by system resistivity  $R_S$ . Thus, even a very low harmonic component in the supply voltage aligned with the series resonant frequency will cause a very large harmonic current. Consequently, the harmonic voltage at the compensator PCC greatly increases, too.

An analogue derivation can also be applied for the parallel resonance. The equivalent (parallel) impedance of the network for the case of harmonic current source  $I_h$  can be written as (see Fig. 2 b):

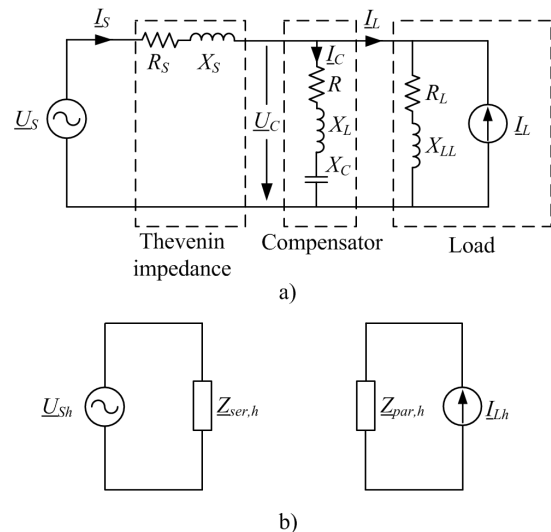


Figure 1. Equivalent circuit of the industrial network; a) single-line diagram, b) series equivalent impedance and parallel equivalent impedance of the network.

$$Z_{par,h} = \frac{\left( j \cdot h \cdot X_{L,1} - j \cdot \frac{X_{C,1}}{h} \right) \cdot (R_S + j \cdot h \cdot X_{S,1})}{\left( j \cdot h \cdot X_{L,1} - j \cdot \frac{X_{C,1}}{h} \right) + (R_S + j \cdot h \cdot X_{S,1})}, \quad (6)$$

$$Z_{par,h} \approx \frac{\left( -j \cdot \frac{X_{C,1}}{h} \right) \cdot (j \cdot h \cdot X_{S,1})}{\left( -j \cdot \frac{X_{C,1}}{h} \right) + (R_S + j \cdot h \cdot X_{S,1})}, \quad (7)$$

$$Z_{par,h} \approx \frac{\left( \frac{X_{C,1}}{h} \right)^2}{R_S} = \frac{(h \cdot X_{S,1})^2}{R_S}, \quad (8)$$

$$Z_{par}^{fr-p} \approx \frac{(X_C)^2}{R_S} = \frac{(X_S)^2}{R_S}. \quad (9)$$

Since  $X_S \gg R_S$ , impedance  $Z_{par}^{fr-p}$  becomes very high near parallel resonance frequency  $f_{r-p}$ . Consequently, even a very low harmonic current can cause a very large voltage drop on equivalent impedance  $Z_{par}^{fr-p}$ . The harmonic voltage component at the compensator PCC will, in turn, greatly increase.

Figure 2 shows a typical frequency response of a network with one compensator. The characteristics are given as an amplification of impedance value relative to the impedance value at 50 Hz. The upper two characteristics are series-frequency characteristics and the lower two are parallel-frequency characteristics. As it can be seen, both the series- and parallel-resonance points are very close to the 5<sup>th</sup> harmonic component with the impedance reaching very low (-26 dB) and very high values (30 dB). In a real industrial network this would most certainly cause high values of the voltage and current total harmonic distortion (THD).

Thus, in order to prevent resonance amplifications of the harmonics present in a network, the central algorithm is needed to ensure that the resonance points (series and parallel) do not align with the harmonics present in the network, for which the resonance points have to be calculated for every harmonics-producing load.

### 3 VIRTUAL COMPENSATOR

Figure 3 shows the basic concept of the proposed virtual compensator. The proposed algorithm is of a central type. The main idea is to combine all the devices contributing to the reactive-power control (compensators, distributed generation units), in a single control scheme implemented on a central computer in the industrial-network control centre. This allows for independent controlling of each compensator in real time and to achieving of an optimal compensator

configuration for every operation point of the network. As a criterion of optimality, some other parameters, such as power losses, voltage profile, etc., can also be used, besides harmonic amplifications.

As seen from Figure 3, the interfaces between the

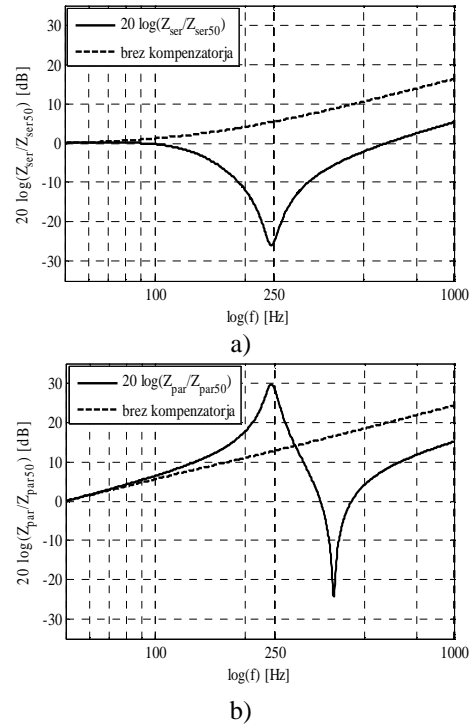


Figure 2. Impedance-frequency characteristics of the network with and without a compensator; a) series impedance, b) parallel impedance.

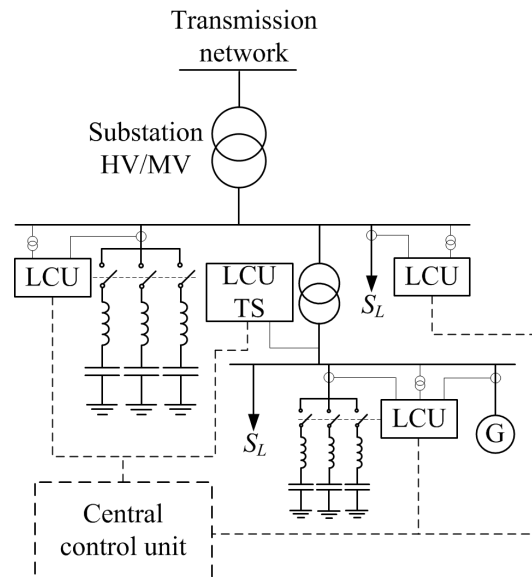


Figure 3. Basic concept of the proposed virtual compensator.

central algorithm and individual devices are local control units (LCU) used in recording measurements of relevant quantities (voltages, currents), monitoring positions of switches, sending data to the control centre and receiving commands for switches settings. Besides these control functions, they also perform protective and other functions.

In the following section, the problem is written in a mathematical form, the objective function is defined and the control algorithm is presented in some detail.

#### 4 PROBLEM FORMULATION

The following equations can be written from Fig. 2 for every voltage-harmonic component  $h$  and current component  $m$  present in the network:

$$A_{h,ser} = k_{ser,h} \cdot \int_{f_h-5Hz}^{f_h+5Hz} |Z(f)_{opt,ser} - Z(f)_{ser}| \cdot df, \quad (10)$$

$$A_{m,par} = k_{par,m} \cdot \int_{f_m-5Hz}^{f_m+5Hz} |Z(f)_{opt,par} - Z(f)_{par}| \cdot df, \quad (11)$$

where  $k_{ser,h}$  and  $k_{par,m}$  are proportional factors describing the harmonic spectrum of the corresponding nonlinear load. For example, for a six-pulse converter, the proportional factors are  $k_h = 1/h$  and  $h = 6i \pm 1$ , where  $i = 1, 2, 3 \dots$ .  $Z(f)_{opt,ser}$  and  $Z(f)_{opt,par0}$  are series and parallel equivalent impedances for no compensator present in the network and for all the loads in the network having  $PF = 0.95$ . These two impedance characteristics are set to be the optimal frequency response of the network.  $Z(f)_{ser}$  and  $Z(f)_{par}$  are actual series and parallel equivalent impedances. As it can be seen from (10) and (11), the absolute value of the difference is then integrated within the limits of  $\pm 5$  Hz from the corresponding harmonic. Terms  $A_{h,ser}$  and  $A_{m,par}$  describe the surface between the optimal and the actual frequency characteristics (series and parallel) in the vicinity of  $\pm 5$  Hz from the corresponding harmonic [1, 11].

The objective function becomes:

$$f = \sum_{i=1}^I S_{loss,i} + \sum_{h=3,5,7\dots} A_{h,ser} + \sum_{j=1}^J \sum_{m=3,5,7\dots} A_{jm,par} \quad (12)$$

s.t.:

$$\begin{aligned} 0.95 &\leq PF_{ind} \leq 1 \\ S_{TR,j} &< S_{r,j} \end{aligned} \quad (13)$$

Here,  $I$  means the total number of branches and  $J$  the number of the harmonic producing loads in the system.  $PF$  is measured at the PCC and  $S_{TR,j}$  is the actual power

flow through the transformer. It must be lower than its rated power  $S_{r,j}$ .

The control algorithm operates according to the following steps:

1. initialisation and data transfer from LCU,
2. setting a new configuration of compensation devices,
3. calculation of the reactive-power requirements, calculation of network losses and calculation of variables, used in the objective function,
4. objective function calculation,
5. verification of objective-function limitations, when any of the conditions is not met, the algorithm returns to the second step,
6. all the configurations having been considered, the algorithm is finished. In the opposite case it is returned to the second step.

The algorithm operates in cycles. Each cycle must be short compared to the time interval defined as the averaging time of the PF value. When determining the duration of a cycle, a compromise has to be achieved between the number of switching operations and achievement of the desired PF. The processing power and the speed at which measurements are performed also strongly affect this value. In solving the nonlinear discrete optimization problem, the Monte Carlo method was employed.

#### 5 THE SYSTEM UNDER STUDY

In Figure 4, a simplified scheme of a real industrial network is shown. The network is powered through a 110 kV transmission system with the short-circuit power of 1200 MVA at PCC. Loads are connected to a dual busbar system on the 20 kV voltage level and to a dual busbar system on the 5 kV voltage level. Under normal operating conditions, an arc furnace and a ladle furnace are connected to the 20 kV busbar system no. II that is powered by two 110/20 kV, 20 MVA transformers (TR V and TR VI). Other loads in the system are connected to the busbar system no. I on the 20 kV and at 5 kV voltage level. This part of the network is powered through a 40 MVA triple-winding transformer TR VII as shown in Fig. 4. On the 5 kV voltage level, there operate three cogeneration units of the rated power of 2.7 MVA.

There are more than 20 passive compensators operating in the network, i.e. C1 and C2 on 20 kV, C3 on 5 kV and several smaller compensators on 0.4 kV. The compensators on the 0.4 kV voltage level were divided into three groups: G1 ranging from 0.4 to 0.48 MVar (the total of 2.147 MVar), G2 from 0.52 to 0.65 (the total of 6.7 MVar), MVar and G3 from 0.8 to 1.2 MVar (the total of 2.887 MVar). Some data for individual compensators are provided in Table 1.

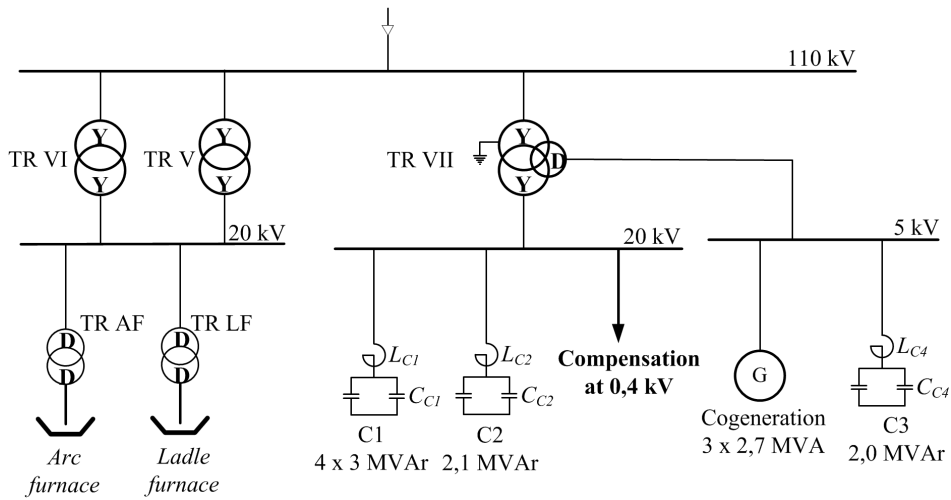


Figure 4. Simplified single-line diagram of real industrial network.

### 6 RESULTS AND DISCUSSION

Results are shown for a typical operating point of the power network. As seen from Fig. 5, 49 combinations of compensators fulfil the set limitations. Their PF is within the limits of 0.95 and 1 (Fig. 7) and no transformer is overloaded. Fig. 6 shows network losses for each of the 49 configurations. As one can see, the lowest losses are by some 15 % lower than the highest losses.

Table 1: Rated data of passive compensators.

Compensator	Rated voltage (kV)	Rated power (MVar)	Reactance (mH)
C1	20	4 x 3	3.63
C2	20	2.1	24.98
C3	5	2	0.100
G1-G3	0.4	0.4 – 1.2	/

The objective function reaches its lowest value when compensators operate as follows (combination no. 4 – circled with a dashed line): compensator C1 with 3 MVar, C2 with 2.1 MVar and C3 not in operation. All the compensators in G2 (6.7 MVar) and G3 (2.887 MVar) are connected, while the compensators in G1 (2.147 MVar) are disconnected. The worst case occurs when the compensators are arranged as follows (combination no. 47 – circled with full line): C1 operates with 12 MVar, C2 with 2.1 MVar, C3 with 2 MVar and other compensators are disconnected.

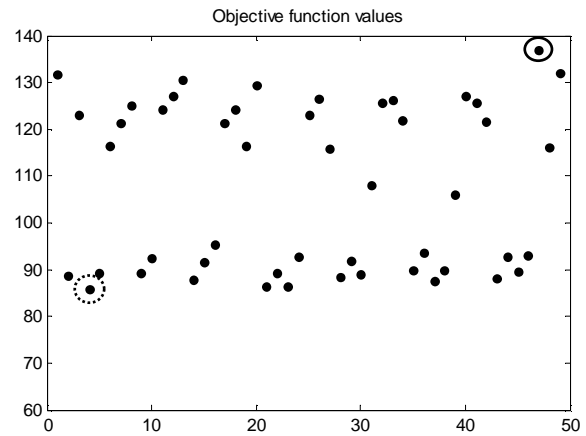


Figure 5. Objective-function values for 49 combinations.

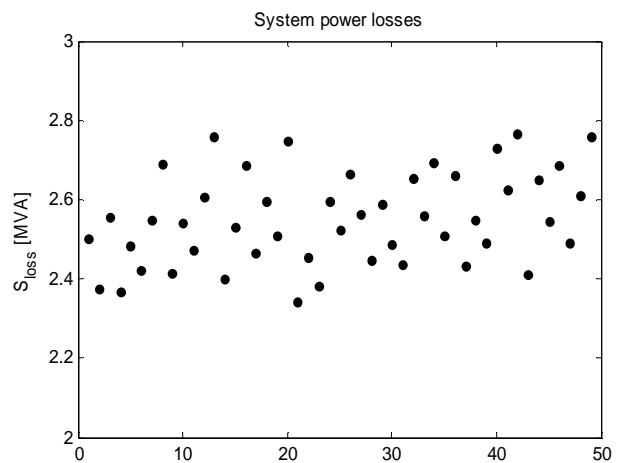


Figure 6. System power losses.

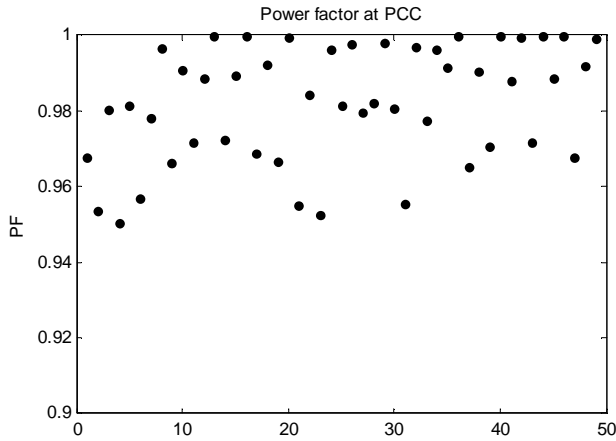


Figure 7. Power-factor values at PCC.

Figs. 8-10 and Figs. 11-13 show the impedance frequency characteristics (series and parallel) for an optimal combination of compensators and for the worst case, respectively. In both cases, the equivalent impedance values are shown relative to the value of the impedance at 50 Hz. The characteristics for the case with no compensator connected are shown with dashed lines.

Note that the y-axis is in the logarithmic scale and that the series equivalent impedance was calculated from the supply voltage point on the 110 kV voltage level and the parallel impedances from the load sides at 20 kV and 5 kV. The harmonic components present in the studied network are of the 3<sup>rd</sup>, 5<sup>th</sup>, 7<sup>th</sup>, 11<sup>th</sup> and 13<sup>th</sup> order.

Figs. 8-10 show that there is no significant amplification of harmonics. The case in Figs. 11-13 showing the worst case characteristics is the opposite. As seen from Fig. 13, there is a resonance point close to the 7<sup>th</sup> harmonic. The equivalent impedance reaches 42 times the value of the impedance at 50 Hz (75 dB), while in the optimal case, it reaches only 4 times (28 dB) this value (see Table 2).

Table 2: Equivalent impedance values at certain harmonic orders for the optimal and worst case.

[dB]	3 <sup>RD</sup>	5 <sup>TH</sup>	7 <sup>TH</sup>	11 <sup>TH</sup>	13 <sup>TH</sup>
Optimal $Z_{ser}$	-9.8	-26.7	-15.5	-2.3	1.8
Optimal $Z_{par1}$	17.6	13.1	-18.8	15.9	22.2
Optimal $Z_{par2}$	19.9	19.9	28.8	39.9	43.6
Worst case $Z_{ser}$	-20.4	-19.8	-14.3	1.8	5.8
Worst case $Z_{par1}$	8.3	-4.6	19.1	24.1	28.9
Worst case $Z_{par2}$	20.8	35.1	75.1	23.2	12.9

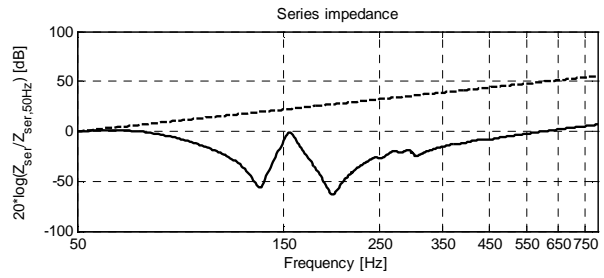


Figure 8. Impedance-frequency characteristics for an optimal combination – series impedance.

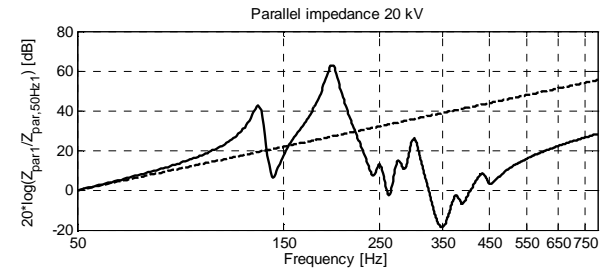


Figure 9. Impedance-frequency characteristics for an optimal combination – parallel impedance on the 20 kV voltage level.

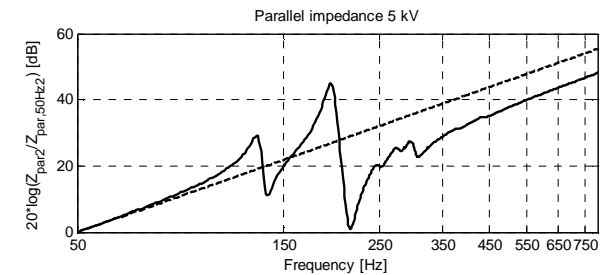


Figure 10. Impedance-frequency characteristics for an optimal combination – parallel impedance on the 5 kV voltage level.

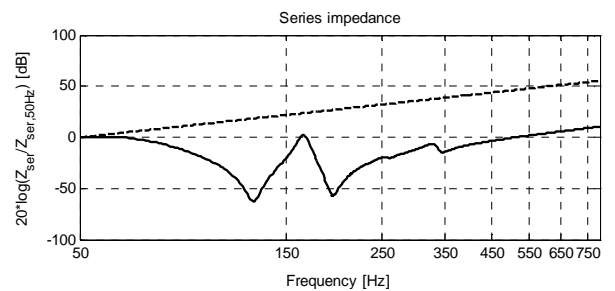


Figure 11. Impedance-frequency characteristics for the worst case – series impedance.

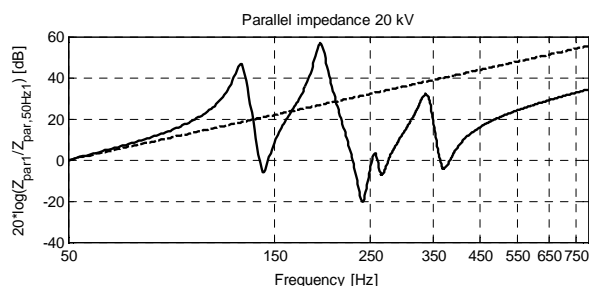


Figure 12. Impedance-frequency characteristics for the worst case – parallel impedance on the 20 kV voltage level.

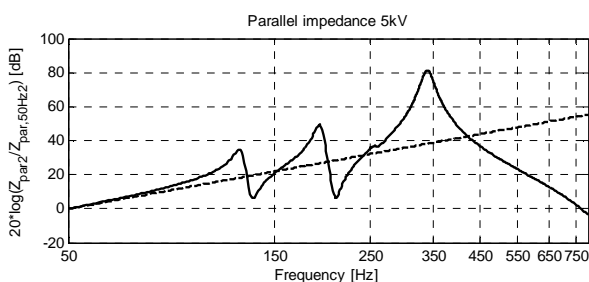


Figure 13. Impedance-frequency characteristics for the worst case – parallel impedance on the 5 kV voltage level.

## 7 CONCLUSION

By introducing the presented virtual-compensator concept, the reactive-power compensators in industrial networks are controlled and resonance amplifications of harmonics are prevented. At the same time, we achieve minimal system power losses and transmission capacity release.

Effectiveness of the proposed algorithm was demonstrated with the simulations made on a realistic industrial network model. The results show that the proposed algorithm can be used in finding the optimal configuration of compensation devices.

## ACKNOWLEDGEMENTS

The work was financially supported by the Slovenian Research Agency under the Electrical Power Systems Research Program no. P2-356.

## REFERENCES

- [1] R.C. Dougan, M.F. McGranaghan, S. Santoso, H.W. Beaty, *Electrical Power Systems Quality*, McGraw-Hill, 2002.
- [2] IEEE Guide for Application of Shunt Power Capacitors, IEEE Standard 1036-1992, 1992.
- [3] Ng, H.N.; Salama, M.M.A.; and Chikhani, A.Y.; "Classification of capacitor allocation techniques," *IEEE Transactions on Power Delivery*, Vol. 15, No. 1, pp. 387-392, January 2000.
- [4] Fawzi, T.H.; El-Sobki, S.M.; and Abdel-Halim, M.A.; "New approach for the application of shunt capacitors to the primary distribution feeders," *IEEE Transactions on Power Apparatus and Systems*, Vol. 102, No. 1, pp. 10-13, Jan. 1983

- [5] Abdel-Salam, T.S.; Chikhani, A.Y.; and Hackam, R.; "A new technique for loss reduction using compensating capacitors applied to distribution systems with varying load condition," *IEEE Transactions on Power Delivery*, Vol. 9, No. 2, pp. 819-827, Apr. 1994.
- [6] Chin, H.C.; "Optimal shunt capacitor allocation by fuzzy dynamic programming," *Electric Power Systems Research*, Vol. 35, pp. 133-139, 1995.
- [7] Baghzouz, Y.; "Effects of nonlinear loads on optimal capacitor placement in radial feeders," *IEEE Transactions on Power Delivery*, Vol. PD-6, No. 1, pp. 245-251, January 1991.
- [8] Masoum, M.A.S.; Ladjevardi, M.; Jafarian, M.; and Fuchs, E.F.; "Optimal placement, replacement and sizing of capacitor banks in distorted distribution networks by genetic algorithms," *IEEE Transactions on Power Delivery*, Vol. 19, No. 4, October 2004.
- [9] Chin, H.C.; "Optimal shunt capacitor allocation by fuzzy dynamic programming," *Electric Power Systems Research*, Vol. 35, pp. 133-139, 1995.
- [10] Wu, Z.Q.; and Lo, K.L.; "Optimal choice of fixed and switched capacitors in radial distributions with distorted substation voltage," *IEE Proceedings on Generation, Transmission and Distribution*, Vol. 142, No. 1, pp. 24-28, January 1995.
- [11] J. Arrillaga, D. A. Bradley, P. S. Bodger, *Power System Harmonics*, John Wiley & Sons, 1985.

**Leopold Herman** (S'08) received his B.Sc. Degree in Electrical Engineering from the Faculty of Electrical Engineering of the University of Ljubljana, Slovenia, in 2008. Currently, he is a Researcher at the same faculty. His research interests include power quality and power system simulations.

**Igor Papič** (S'97-A'99-M'00-SM'06) received his B.Sc., M.Sc. and Ph.D. degrees in Electrical Engineering from the Faculty of Electrical Engineering of the University of Ljubljana, Slovenia, in 1992, 1995 and 1998, respectively. From 1994 to 1996, he was with Siemens Power Transmission and Distribution Group in Erlangen, Germany. Currently, he is a Professor at the same faculty. In 2001, he was a Visiting Professor at the University of Manitoba, Winnipeg, Canada. His research interests include power conditioners, FACTS devices, power quality and active distribution networks.